Nanoscale

PAPER

View Article Online
View Journal

Cite this: DOI: 10.1039/d6nr00796a

Tea polyphenols increase nanoplastic release from plastic cups but mitigate potential detrimental effects during simulated tea drinking

Haoxin Ye, David D. Kitts, Xiwen Wang, Tianyu Wang, Yifan Wang and Tianxi Yang *

The presence of micro- and nanoplastics (MNPs) in daily life raises increasing concerns about their potential health and environmental impacts. However, how food components influence MNP release from packaging materials and the resulting exposure risks remain poorly understood. Here, we investigated the effect of the primary tea polyphenol, epigallocatechin gallate (EGCG), on MNP release from polystyrene cups during a simulated tea-drinking process involving thermal treatments. A surface-enhanced Raman scattering sensor was developed to quantify released plastic particles *in situ* using EGCG-based luminescent metal–phenolic network labeling. The released particles were identified primarily as nanoplastics, and the presence of EGCG significantly ($P < 0.05$) increased MNP release, particularly during microwave heating and most prominently upon repeated cup use. Interestingly, EGCG increased the MTT response of differentiated Caco-2 cells exposed to released NPs in a dose-dependent manner, suggesting a potential mitigation of NP-associated cytotoxicity under the tested *in vitro* conditions. This study provides new insight into the dynamic interactions between food components and plastic packaging during realistic consumption scenarios, revealing an overlooked pathway influencing human exposure to nanoplastics. The findings expand the current understanding of contaminant release mechanisms at the food–environment interface and inform future strategies for exposure mitigation and sustainable material design to ensure food safety and protect environmental and public health.

Received 26th February 2026,
Accepted 16th May 2026

DOI: 10.1039/d6nr00796a

rsc.li/nanoscale

Introduction

The practice of using plastics in many aspects of daily consumer activities, ranging from purchasing clothing and healthcare products to including a variety of packaged commodities used to increase shelf-life and food safety, is an ongoing practice in today's reality. The omnipresence of micro/nanoplastics (MNPs) has resulted in an increased awareness of the consequences to ecological and environmental issues that relate to pollution of both land and sea habitats. It is estimated that 4.8 to 12.7 million tons of plastic enter the oceans annually; however, the magnitude of plastic emissions on land and into freshwater systems is significantly higher, thus posing an even greater environmental challenge.[1] A pressing concern is the transformation of conspicuous plastic waste derived from agricultural, food, and environmental systems into microplastics (MPs, with sizes ranging from 1 μm to 5 mm) and nanoplastics (NPs, smaller than 1 μm).[2] This process of release into the environment is facilitated by mechanical stress and photochemical, thermal, and biological decomposition; processes that fracture the plastic into smaller, more pervasive fragments.[3] These particles can readily disperse into ecosystems and water bodies, potentially on exposure, leading to a variety of human health issues that involve oxidative stress, cellular damage, inflammation, DNA damage, neurotoxic effects, and overall metabolic disturbances.[4,5]

Contemporary techniques for identifying and measuring MNPs typically utilize microscopic and spectroscopic approaches, such as scanning electron microscopy (SEM) and pyrolysis mass spectrometry (MS).[6–8] Despite the effectiveness of these procedures, significant challenges exist to increase the efficiency of establishing an accurate risk assessment. High costs, labor-intensive procedures, and the need for skilled operators are recognized hurdles that must be overcome for the adoption of rapid screening techniques.[9–11] Recent advances in rapid screening applications, such as smartphone-based fluorescence microscopy and handheld surface-enhanced Raman scattering (SERS) assays, can provide fast, on-the-spot, alternative methods of analysis. However, they, too, are hindered by a relatively lower sensitivity, thus reducing applicability in real-life situations.[12,13] Our prior research reported the development of an L-MPN-assisted SERS platform

Food, Nutrition and Health, Faculty of Land and Food Systems, The University of British Columbia, Vancouver V6T1Z4, Canada. E-mail: tianxi.yang@ubc.ca

for the rapid and sensitive detection of plastic particles, which provides the basis for the EGCG-based adaptation used in the present study.[14] L-MPNs, a novel labeling system composed of phenolic ligands, metal ions, and conventional dyes, were successful in facilitating a rapid (<5 minutes) labeling process for various plastic particles.[15] The robust Raman signals generated by the dyes used in our process allowed them to serve as Raman reporters, thereby enhancing sensitivity by up to 500 times, equivalent to an unprecedentedly low detection limit of 0.1 ppm for polystyrene (PS).[14] This innovative approach has significant promise for use to assess real-world plastic contamination scenarios.

Understanding the dynamics of exposure to MNPs in the food environment is a crucial step for mitigating potential risks to human health. Such exposures can occur through skin contact, inhalation, or ingestion, including seemingly benign activities such as drinking hot tea from plastic cups. Previous research has shown that the interaction of heat with plastic containers undeniably leads to the release of plastics into hot beverage fluids.[16] For example, plastic teabag studies demonstrated that brewing at 95 °C can release extremely large quantities of micro- and nanoplastics into tea, highlighting hot beverages as a realistic exposure route.[17] Although recent studies have shown that green tea extracts and catechin-rich systems can induce microplastic aggregation, reduce bioaccessibility, and suppress intestinal transport *in vitro*,[18] little is known about whether a specific tea polyphenol can influence the release of plastic particles from food-contact materials during beverage preparation or modify the subsequent biological response. Tea catechins, particularly epigallocatechin gallate (EGCG), are present in green tea and black tea and have well-known bioactive antioxidant and anti-inflammatory activities.[19,20] In addition to tea beverages, EGCG is also found in a range of different food products packaged in plastic containers, including dried fruits and nuts.[21,22] The relationship between EGCG and the release of plastic particles requires further investigation to understand potential implications for human health. Moreover, EGCG was selected in this study not to suggest a general performance advantage over other polyphenols (*e.g.*, tannic acid), but because it uniquely serves a dual role in this food-relevant model system: as a representative tea polyphenol that may influence nanoplastic release and as a phenolic ligand capable of forming L-MPNs through coordination with metal ions and π–π interactions with dyes. By integrating an EGCG-based L-MPN labeling approach with our previously developed SERS platform, we achieved *in situ* monitoring of MNPs released from plastic cups within the same chemically relevant exposure scenario.

In this research, EGCG was selected not only for being a representative bioactive tea polyphenol,[20] but also as a phenolic ligand candidate to form L-MPNs for SERS quantification of released plastic particles (Scheme 1). The novelty of this study is (i) applying an EGCG-based L-MPN labeling system to this specific PS cup model, (ii) revealing that EGCG can significantly influence nanoplastic release under simulated tea-drinking thermal conditions, and (iii) integrating release quantification with a preliminary biological-response assessment in differentiated Caco-2 cells. These results provide novel insights into contaminant release dynamics, exposure risk assessment, and the need for safer, more sustainable materials in food contact applications.

Experimental

Materials

Polystyrene nanoplastics with a particle size of 500 nm were purchased from Phosphorex (Massachusetts, USA). EGCG (pharmaceutical secondary standard) and zinc chloride ($ZnCl_2$, >98%) were purchased from Sigma-Aldrich (Ontario, Canada). Rhodamine B (ACS reagent ≥99%) was purchased from VWR (Alberta, Canada). Dulbecco's Modified Eagle's

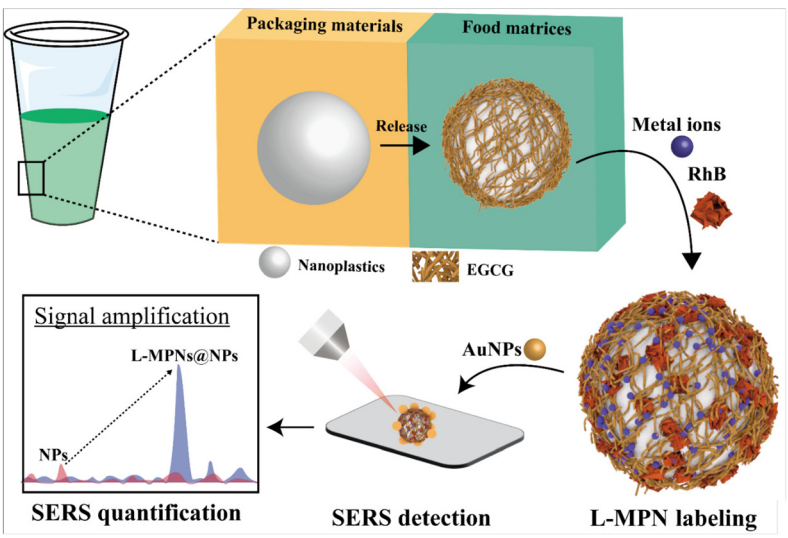

Scheme 1 Nanoplastic release and subsequent SERS detection during simulated tea drinks.

Medium (DMEM-D5796; without pyruvate), phosphate buffered saline (PBS), penicillin/streptomycin antibiotics, 3-(4,5-diethylthiazol-2-yl)-2,5-diphenyltetrazolium bromide (MTT) and dimethyl sulfoxide (DMSO) were purchased from Sigma (St Louis, MO, USA). Fetal bovine serum (FBS) was purchased from Gibco® (Grand Island, NY, USA). Transparent commercial polystyrene drinking cups (Ruisita, ASIN, B0B3GTSH4D) were purchased from Amazon.ca. The capacity of these clear mini dessert cups is 3 ounces; the dessert cups measure 3.1 inches/8 cm in height, 1.9 inches/4.7 cm in top diameter, and 1.3 inches/3.2 cm in bottom diameter. Gold nanoparticles (AuNPs, 50 nm ± 4 nm at a concentration of 1 mg L^{-1}) were purchased from nanoComposix (San Diego, CA, USA). Double-distilled water (DD water) was produced using a distillation system in the Food, Nutrition and Health building at the University of British Columbia (UBC), Vancouver campus.

Preparation of L-MPNs@NPs

EGCG, Zn^{2+} metal ions, and RhB were selected as model reagents for the formation of L-MPNs. The preparation of L-MPN-labeled nanoplastics (L-MPNs@NPs) was carried out according to the protocols described in our prior research.[23] 500 nm PS NP solutions were prepared to various concentrations of 0, 1.54×10^7, 7.7×10^7, 1.54×10^8, 7.7×10^8, 1.54×10^9, 7.7×10^9, 1.54×10^{10}, 7.7×10^{10}, and 1.54×10^{11} n mL^{-1}. The nanoplastic concentration was provided by Phosphorex and further validated in our previous study using electrophoretic deposition–interferometric scattering (EPD-iSCAT).[24,25] Subsequently, EGCG was added into these suspensions to achieve a final concentration of 1 mg mL^{-1}. For the labeling process, 20 μL of $ZnCl_2$ (20 mM) and 20 μL of RhB (0.5 mM) were added to 960 μL of NPs–EGCG mixture, resulting in final concentrations of 400 μM Zn^{2+} and 10 μM RhB. This mixture was thoroughly vortexed for 1 min and then centrifuged at 7500 rpm for 10 min. The supernatant was removed, and the precipitate was resuspended in 1 μL of DD water to prepare L-MPNs@NPs.

Characterization of L-MPNs@NPs

L-MPN labeling on NPs was characterized using dynamic light scattering (DLS) and fluorescence measurements. DLS assessments for released NPs and L-MPNs@NPs samples were performed with a Litesizer 500 (Anton Paar, Graz, Austria). Fluorescence spectroscopy measurements were performed with a Tecan Infinite 200Pro plate reader (excitation at 550 nm; emission at 595 nm) for released NPs labeled with RhB, Zn^{2+}/RhB, EGCG/RhB, and L-MPNs. Transmission electron microscopy (TEM) imaging was examined under a Hitachi H7600 TEM (Tokyo, Japan) at 80 kV for released NPs and NPs–EGCG mixtures.

Detection of NPs by SERS

SERS was utilized to determine NPs labeled with L-MPNs. An AuNP solution was prepared by diluting a stock solution to 0.5 mg mL^{-1} with DD water. A 1 μL droplet of AuNP solution was applied onto aluminum foil, followed by the addition of an equal volume of the L-MPNs@NPs samples. Samples were allowed to air dry at room temperature for 10 min. Subsequently, SERS spectra were acquired at the periphery of the resultant coffee ring using a WP 785 ER Raman spectrometer, which is equipped with a 785 nm excitation laser. The most reproducible signal from each sample was selected as the representative spectrum. Spectral acquisition was conducted under controlled conditions: the laser was set to a power of 450 mW, the integration time was fixed at 60 s, and spectra were recorded continuously over a range of 300–2008 cm^{-1}. The spectral data were processed using boxcar smoothing and polynomial baseline corrections to enhance the signal clarity for improved accuracy.

MNP release in a simulated tea consumption process

EGCG was chosen as the representative bioactive polyphenol to simulate a simplified tea drink. The study utilized two primary thermal processes: boiling water and microwave heating water, with a cold water control. For the boiling water treatments, different concentrations of EGCG (*e.g.*, 0.1, 0.2, 0.4, and 0.6 mg mL^{-1}) were added. In the microwave experiments, EGCG at the same concentrations used above was added to DD water at room temperature, followed by exposure to microwave heating (900 W) at varying time durations (*e.g.*, 0, 15, 30, 60, 90, 120, 150, and 180 s). Following heating, all samples were cooled naturally at room temperature for approximately 30 min. The EGCG concentrations were adjusted to 1 mg mL^{-1} to maintain consistency across all samples. Subsequently, the release of NPs was measured by preparing L-MPNs@NPs and then using SERS for quantification analysis.

Caco-2 cell viability exposed to NPs and NPs with EGCG

Twenty-one-day-old differentiated Caco-2 cells were used in this study to test the potential toxicity of NPs recovered from the plastic cups containing hot water. Cells were cultured in Dulbecco's modified Eagle's medium (DMEM) containing 4500 mg L^{-1} glucose and sodium bicarbonate, without L-glutamine and sodium pyruvate. Cell media also contained 10% FBS (Invitrogen, Canada) and 100 U mL^{-1} penicillin and 100 μg mL^{-1} of streptomycin (PS). Cells were cultured at 37 °C under a controlled atmosphere with 5% CO_2. The passage number for Caco-2 cells used in these experiments was 21–30. Caco-2 cells were seeded into 96-well plates at a density of 1×10^5 cells per cm^2, and the cell culture media were changed every 2–3 days for 21 days until differentiation.

Redox activity was assessed in differentiated Caco-2 cells as a measure of viability using the MTT assay (3-(4,5-dimethylthiazol-2-yl)-2,5-diphenyltetrazolium bromide) in 96-well plates. This assay is based on a redox mechanism, whereby NADPH-dependent enzymes in viable, healthy cells reduce MTT to formazan crystals, which are quantified by spectrophotometry.[26] The cells were first incubated with NPs and EGCG (0.1, 0.2, 0.4, and 0.6 mg mL^{-1}) in cell culture medium. A positive control consisted of using NPs (1.54×10^6, 1.54×10^7, 1.54×10^8 and 1.54×10^9 n mL^{-1}) present with no EGCG. After 24 h

of incubation, Caco-2 cells were washed with 100 μL of phosphate-buffered saline (PBS) three times and then incubated with 100 μL of DMEM containing 0.5 mg mL^{-1} MTT for 4 h in the dark at 37 °C. Dimethyl sulfoxide (DMSO, 100 μL) was then added to the wells without discarding the DMEM, allowing formazan crystals to dissolve (for measuring the absorbance) with another 30 min. The solubilized formazan in the wells was quantified by measuring absorbance at 540 nm, using the Multiskan SkyHigh Spectrophotometer (Thermal Fisher, Chantilly, VA, USA) with the following equation:

$$\text{Viability (shown as \% of control)} = \frac{\text{Abs}_{\text{sample}}}{\text{Abs}_{\text{control}}} \times 100\%$$

where $\text{Abs}_{\text{sample}}$ is the absorbance of cells that received treatment, and $\text{Abs}_{\text{control}}$ is the absorbance of the cells that did not receive treatment (negative control).

Statistical analysis

All experiments were performed using at least three technical replicates unless otherwise stated, and results are reported as mean ± standard deviation (SD). Statistical analyses were performed using OriginPro 2021 (OriginLab, Northampton, MA, USA). Comparisons between two groups were conducted using a two-tailed Student's *t*-test, and differences were considered statistically significant at $P < 0.05$. For SERS quantification, a polynomial regression model was used to generate the calibration curve relating the nanoparticle concentration to the characteristic Raman peak intensity. The uncertainty reported in this study is based on the variability among replicate measurements; formal error propagation across the full analytical workflow, including calibration-model fitting and sample-processing steps, was not performed in the present study.

Results and discussion

Formation of L-MPNs@MNPs

The L-MPN labeling strategy can be applied to PS plastic particles through a straightforward and simple self-assembly process.[14] For example, in our previous research, tannic acid/zirconium metal ions/RhB-based L-MPNs were used to effectively quantify commercial 500 nm PS NPs employing SERS measurements. In this study, we used EGCG and Zn^{2+} as model reagents to form L-MPNs on released MNPs from polystyrene cups. EGCG was chosen not to imply that it is generally superior to other polyphenols (*e.g.*, tannic acid) for L-MPN formation, but because it allows the same food-relevant polyphenol to function both as a release-active component in the simulated tea system and as a ligand in the sensing platform. Fig. 1a depicts plastics released from commercial plastic cups subjected to microwave heating for 90 seconds. The TEM image illustrates an amorphous morphology for particle sizes ranging from the micro- to the nano-scale. Subsequent fluorescence characterization (Fig. 1b) of RhB interaction with the released plastic particles showed a significant reduction in fluorescence intensity when released MNPs were labeled with RhB, EGCG/RhB, and RhB/Zn^{2+}, in comparison with the labeling with L-MPNs ($P < 0.05$). This result underscores the critical role of the L-MPN coordination network in enhancing fluorescence labeling efficiency. DLS measurements provided additional information on the particle size distribution of the MNPs before and after labeling with L-MPNs, indicating that released particles were primarily in the nanosized range. With post-labeling, a notable shift in the peak particle size from 307 nm to 586 nm occurred (Fig. 1c), which was indicative of successful aggregation facilitated by the L-MPNs. Although micro-sized plastic particles were detected, the predominant fraction consisted of nanoparticles in the range of hundreds of nanometers, with a maximal intensity at 586 nm. Consequently, for SERS optimization and measurement, the released plastic particles were categorized as nanoplastics (NPs) with a size distribution centered around hundreds of nanometers.

SERS measurements of L-MPNs@NPs

To evaluate the efficacy of EGCG-based L-MPNs to quantify NPs utilizing SERS techniques, a series of SERS analyses was

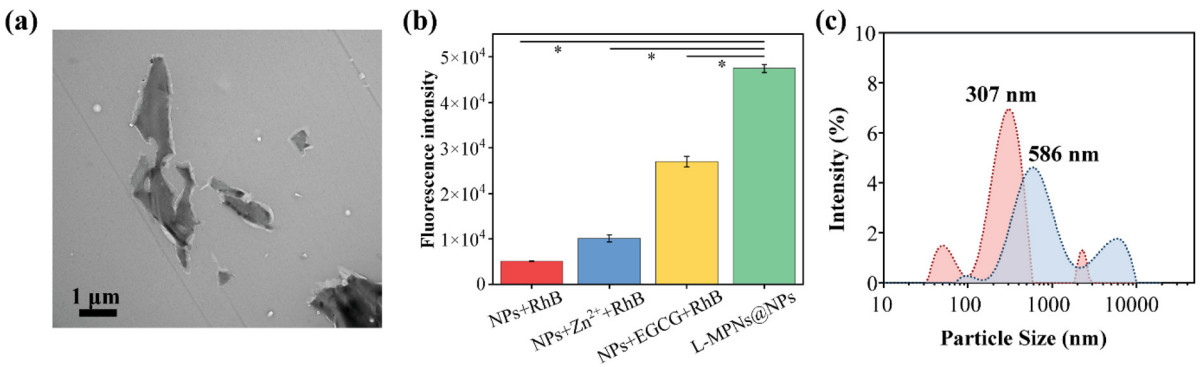

Fig. 1 L-MPN labeling of micro/nanoplastics. (a) TEM image of released plastic particles from plastic cups with microwave heating at 90 s and (b) fluorescence intensity measurements of released plastic particles labeled with RhB, Zn^{2+}/RhB, EGCG/RhB, and L-MPNs. (c) Particle size changes following the formation of L-MPNs@MNPs, in comparison with released MNPs alone. Data are represented as mean ± SD (n = 3 technical replicates). The asterisk (*) indicates a statistically significant difference ($P < 0.05$), as determined using the *t*-test.

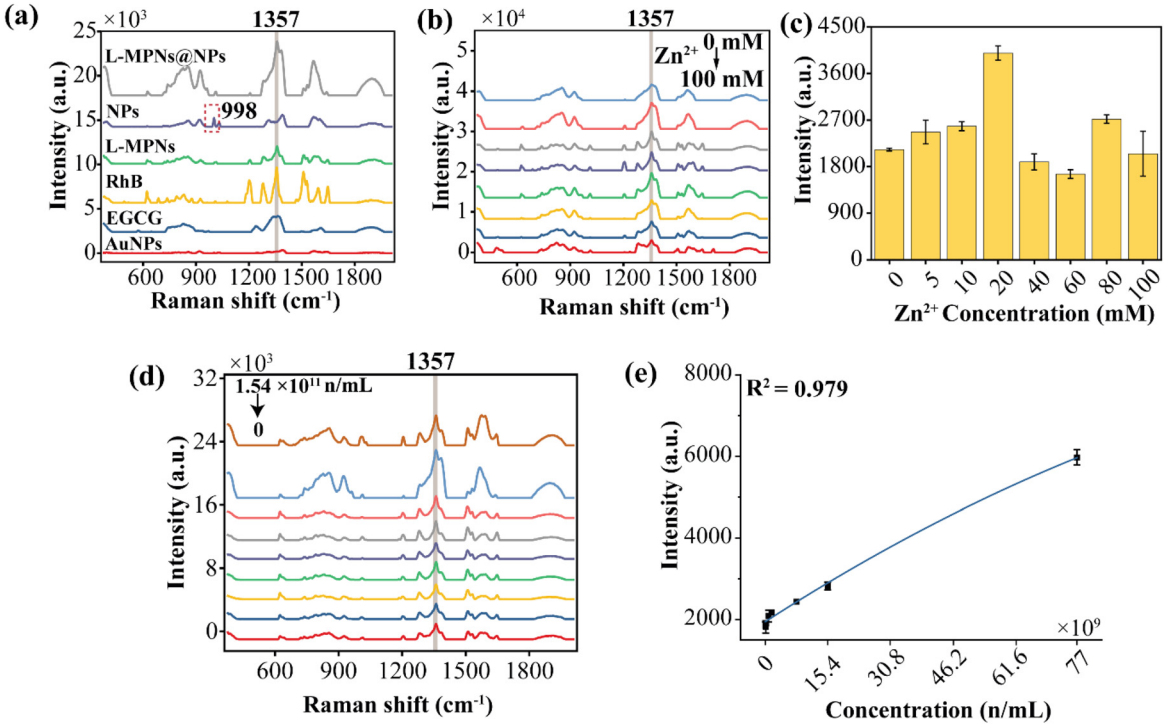

Fig. 2 Optimization and quantitative analysis of nanoplastics *via* SERS measurements. (a) SERS spectra of AuNPs, EGCG, RhB, PS NPs, L-MPNs, and L-MPNs@NPs. (b) SERS spectra of L-MPNs@NPs with various Zn^{2+} concentrations (0, 5, 10, 20, 40, 60, 80, and 100 mM). (c) Variation in the intensity of the characteristic peak at 1357 cm^{-1} for L-MPNs@NPs across these different Zn^{2+} concentrations. (d) SERS spectra of L-MPNs@NPs across various NP concentrations (0, 1.54 × 10^7, 7.7 × 10^7, 1.54 × 10^8, 7.7 × 10^8, 1.54 × 10^9, 7.7 × 10^9, 1.54 × 10^{10}, 7.7 × 10^{10}, and 1.54 × 10^{11} n mL^{-1}). (e) Investigation of the relationship between the concentration of NPs and the SERS characteristic peak intensity at 1357 cm^{-1} from L-MPNs employing a polynomial regression model. The 500 nm PS NP concentration was controlled at 1.54 × 10^9 n mL^{-1} in (a)–(c). Data are represented as mean ± SD (*n* = 3 technical replicates).

conducted on both components (L-MPNs and NPs), both pre- and post-labelling with L-MPNs (Fig. 2a). AuNPs served as the substrate for SERS, which was selected for environmental stability,[27] and PS NPs (500 nm) were chosen to represent NPs according to a known particle size, which closely approximated the plastics released from PS cups, as shown in Fig. 1c. In the spectral analysis, AuNPs exhibited negligible signals across the spectrum. In contrast, RhB had distinctive peaks located at 1201, 1277, and 1357 cm^{-1}, respectively, with a very pronounced peak occurring at 1357 cm^{-1}, indicative of C–C stretching vibrations.[28] EGCG showed two peaks at 1340 and 1362 cm^{-1}, respectively, due to C–O vibrational modes.[29] The PS NPs displayed a characteristic peak at 998 cm^{-1}, attributed to ring-breathing modes. The synthesis of L-MPNs induced alterations in these peak patterns, which were due to molecular interactions between RhB, EGCG, and Zn^{2+}, and attributed to coordination bonding between EGCG and Zn^{2+} and π–π interaction between RhB and EGCG.[30] However, the prominent peak presented at 1357 cm^{-1} was maintained, which served as the characteristic peak of L-MPNs for further quantitative analysis. Upon forming L-MPNs@NPs, the characteristic peak of PS at 998 cm^{-1} was substituted by a peak from the L-MPNs with an enhanced intensity at 1357 cm^{-1}. This finding showed the effectiveness of using RhB as a Raman reporter in EGCG based L-MPNs for improving the sensitivity of SERS detection of NPs.

Subsequent experiments to optimize Zn^{2+} concentrations were conducted to determine the pivotal role of metal ions in the efficacy of L-MPN labeling.[14] Spectral analyses of L-MPNs@NPs (500 nm PS NPs at 1.54 × 10^9 n mL^{-1}) with varying Zn^{2+} concentrations were based on the intensity of the characteristic peak appearing at 1357 cm^{-1} (Fig. 2b). The intensity of this peak was contrasted against control signals derived from L-MPNs without NPs, thus showing the effective SERS signal attributable to the presence of NPs (Fig. 2c). This optimization experiment revealed that increasing the Zn^{2+} concentration produced an enhancement in peak intensity. Low Zn^{2+} concentrations (0–10 mM) were insufficient for effective L-MPN formation on NPs, whereas higher Zn^{2+} concentrations (40–100 mM) facilitated a denser coating, which facilitated greater binding activity with RhB molecules.[31] Excessive RhB binding caused aggregation and interfered with the optimal interaction between the RhB molecules and the SERS substrate (AuNPs), hence diminishing the SERS signal intensity. The Zn^{2+} concentration was optimized to 20 mM, as this concentration yielded the highest L-MPNs@NPs signal intensity. To ascertain the limit of detection (LOD) for NPs using this optimized EGCG-based L-MPN method, a number of SERS assays

were performed across various NP concentrations. The results indicated a limit of detection (LOD) of 7.7×10^7 particles per mL, demonstrating a statistically significant difference ($P < 0.05$) between the sample group and lower concentration groups (Fig. S1). Values exceeding the LOD for SERS signal intensity showed a positive correlation with increasing NP concentration. A maximum concentration (1.53×10^{10}) resulted in a decrease in SERS intensity, likely due to the inhibition of the resonance Raman effect caused by aggregation.[32] Consequently, concentrations ranging from 7.7×10^7 to 7.7×10^{10} n mL^{-1} were used to establish a standard curve employing a polynomial regression model (Fig. 2d and e, $R^2 = 0.979$), which outperformed linear fitting (Fig. S2, $R^2 = 0.969$). This model was used in the present study as a practical calibration framework for SERS-based quantification of L-MPN-labeled NPs. Orthogonal validation of the underlying quantification strategy was established in our previous work using electrophoretic deposition–interferometric scattering (EPD–iSCAT) measurements, whereas the current study focuses on the EGCG-based application of this platform.[33]

Nanoplastic release from PS cups containing EGCG

Release of NPs from plastic products used for hot beverages has emerged as a potential health risk in daily life.[34–36] Our study investigated NP release from PS cups by varying the pH level from 5 to 9 and the concentration of EGCG, a predominant polyphenol in tea, from 0 to 0.6 mg mL^{-1}.[37] Following the application of both boiling water and water heated using microwave energy, respectively, samples were cooled and then labeled with L-MPNs before being quantified using SERS. We used EGCG in this experiment as both a phenolic ligand for L-MPN formation and a representative tea polyphenol in a simplified tea model designed to isolate its specific contribution; this system does not reproduce the full compositional complexity of brewed tea.[38] The phenolic hydroxyl groups present in EGCG did not show appreciable susceptibility to oxidation when exposed to boiling water and microwave heating conditions, respectively, as indicated by the fact that the efficiency of L-MPN labeling was not impacted (Fig. S3). We maintained a consistent EGCG concentration of 1 mg mL^{-1} across different experimental groups to ensure uniform L-MPN labeling conditions.

We first studied the effect of EGCG concentrations and pH levels on nanoplastic release during boiling water heating. Our results indicate that low concentrations of EGCG (*e.g.*, 0.1 and 0.2 mg mL^{-1}) in cups containing boiling water result in detectable, but minimal NP release ($0.5–1 \times 10^8$ n mL^{-1}) across different pH levels. In contrast, significantly higher ($P < 0.05$) NP release (*e.g.*, $4.26 \pm 0.32 \times 10^8$ n mL^{-1}) was observed when EGCG was present at higher concentrations (*e.g.*, 0.4 to 0.6 mg mL^{-1}) (Fig. 3a and Fig. S4). NP release was not detectable in cold water treatment at 30 min because the released NPs were below the LOD of our sensing method and direct SERS detection without L-MPNs (Fig. S5). The ability of EGCG to facilitate NP release is attributed to the high affinity of catechol or galloyl groups in polyphenols, which can bind with various nanoplastics.[19,39] For example, electron-rich π-conjugated orbitals of aromatic rings in PS facilitate the formation of π–π interactions with polyphenol molecules. Furthermore, polyphenols rich in aromatic groups have hydrophobic interactions with various MNPs, such as PS, polyethylene (PE), polyvinyl chloride (PVC), and polypropylene (PP).[40] Under alkaline conditions (*e.g.*, pH 9), higher concentrations of EGCG (0.6 mg mL^{-1}) resulted in more substantial NP release compared to acidic and neutral conditions. Under alkaline conditions, phenolic hydroxyl groups in polyphenols deprotonate to form phenoxide ions. The deprotonation increases the electron density on the phenoxide ion, potentially enhancing its ability to participate in π–π interactions with PS nanoplastics,[41,42] thereby promoting NP release. TEM images confirmed the interaction between PS and EGCG, further substantiating the enhanced release of NPs (Fig. 3b).

Applying microwave energy to heat water in plastic cups notably leads to higher NP release under neutral conditions (pH 7), compared to boiling water heating (Fig. 3a and c and Fig. S6). This effect can be attributed to the susceptibility of PS polymer chains to break down into smaller fragments, creating microcracks or fissures in the plastic cup that will facilitate leaching of NPs into the water.[43] The effect of EGCG on NP release after 30–60 s exposure to microwave energy was significantly greater than the zero time control, thus denoting a significant interaction ($P < 0.05$) between EGCG concentration and microwave heating time, affecting NP release. Note that our SERS assay could not detect EGCG-facilitated NP release below the LOD in control and with very short 15 second microwave heating. The greatest NP release (*e.g.*, $6.47 \pm 0.11 \times 10^9$ n mL^{-1}) that was facilitated by the presence of EGCG occurred at 0.6 mg mL^{-1}, which also indicated that a higher concentration of EGCG induced more NP release. The analysis results of reusable cups are significant as they reflect real-world tea drinking behaviors, where individuals often refill cups multiple times with hot water. We aimed to understand the implications of such practices for NP release. The findings indicate that reusing PS cups treated with heating reaching boiling showed a linear increase in NP measurements after 4 cycles, followed by a small decline thereafter (Fig. 3d and Fig. S7). Again, this was most likely due to damage to the uniform surface typical of PS cups reused and exposed to repeated boiling treatments.

Potential Caco-2 cell cytotoxicity

Twenty-one-day-old differentiated Caco-2 cells served as a representative *in vitro* model for the human intestinal epithelium, enabling the evaluation of the cytotoxic potential of NPs. In this study, we employed changes in Caco-2 cell redox status to assess cell viability when exposed to NPs derived from 500 nm PS. Our findings in Fig. 4a indicate that low NP concentrations (1.54×10^7 and 1.54×10^6 n mL^{-1}) do not significantly alter cell viability from 100% MTT control. Conversely, higher PS NP concentrations (*e.g.*, 1.54×10^8 and 1.54×10^9 n mL^{-1}) decreased MTT-redox values to $91.46 \pm 3.02\%$ and $82.09 \pm 2.39\%$, respectively ($P < 0.05$). These results

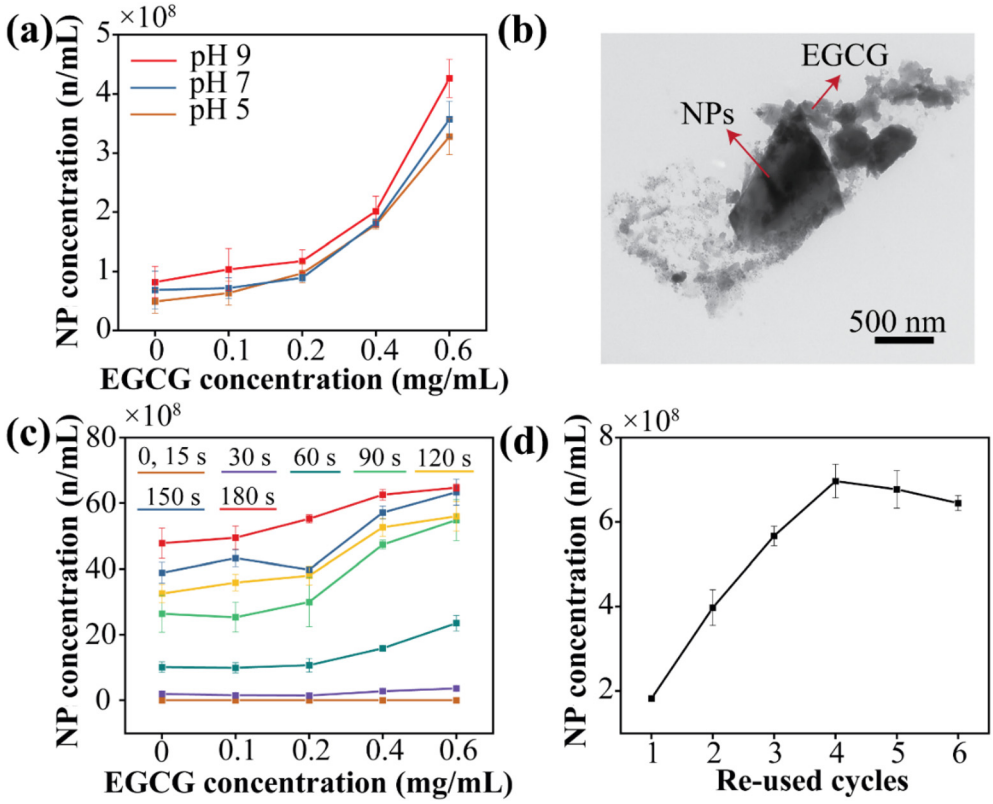

Fig. 3 NP release from water samples containing EGCG. (a) NP release across various EGCG concentrations (0, 0.1, 0.2, 0.4, and 0.6 mg mL^{-1}) and pH conditions (5, 7, and 9) in boiling water. (b) TEM image of released NPs at an EGCG concentration of 0.4 mg mL^{-1}. (c) NP release at different EGCG concentrations (0, 0.1, 0.2, 0.4, and 0.6 mg mL^{-1}) subjected to various microwave heating durations (0, 15, 30, 60, 90, 120, 150, and 180 s). (d) NP release over various reuse cycles. Data are represented as mean ± SD (n = 3 technical replicates). No detectable NPs were recovered from cold water treatments.

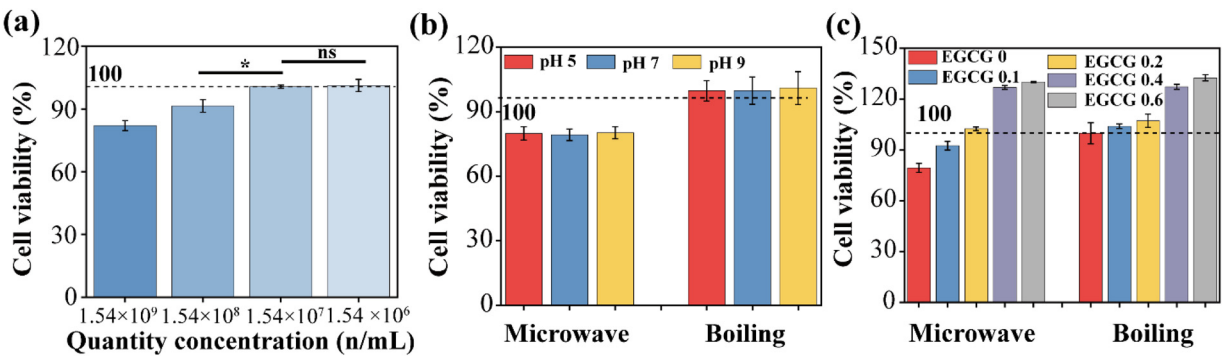

Fig. 4 Influence of PS NPs and EGCG on the viability of Caco-2 cells. (a) Cell viability following exposure to commercially 500 nm PS NPs at concentrations of 1.54 × 10^6, 1.54 × 10^7, 1.54 × 10^8, and 1.54 × 10^9 n mL^{-1}. (b) Cell viability following exposure to released NPs at different pH levels (5, 7, and 9) under microwave heating and boiling conditions. (c) Cell viability following exposure to released NPs at different EGCG levels (0, 0.1, 0.2, 0.4, and 0.6 mg mL^{-1}) under microwave heating and boiling conditions. Data are represented as mean ± SD (n = 3 technical replicates). Values were determined when comparing with cold water control (100%). The label "ns" denotes no significant difference, whereas the asterisk "*" signifies a statistically significant difference with a P-value <0.05, as determined using the t-test.

corroborate previous findings that reported elevated concentrations of NPs are cytotoxic to Caco-2 cells,[44] through mechanisms that are associated with oxidative stress, inflammatory responses, and disruption of cellular functions.[45] The very small size of NPs likely facilitates penetration and accumulation within cellular structures, exacerbating a toxic effect. Examining the effect of pH (*e.g.*, 5–9) on the toxicity of released NPs exposed to microwave heating (90 s) and boiling conditions showed that pH was not a factor in increasing the potential toxicity of NPs (Fig. 4b). Comparing microwave

heating with direct heat boiling showed that the former resulted in a greater release of NPs ($P < 0.05$) and, thus, higher cytotoxicity.

We also explored the potential beneficial effects of adding the tea polyphenol EGCG to potentially reduce Caco-2 cell toxicity under microwave heating and boiling water conditions, respectively. Increasing EGCG concentrations in both heated water treatments significantly enhanced cell MTT responses ($P < 0.05$) (Fig. 4c). EGCG is a known antioxidant capable of scavenging reactive oxygen species and modulating cellular redox balance; in addition, its phenolic structure enables interactions with nanoplastics (*e.g.*, π–π interactions and surface adsorption), which may alter particle surface properties and reduce their biological interactions.[46] When PS cups were microwaved, NP release in heated water occurred and low concentrations (0.1 mg mL^{-1}) of EGCG were insufficient to mitigate the cytotoxic effects induced by NPs. However, at higher concentrations of EGCG (0.2, 0.4, and 0.6 mg mL^{-1}), Caco-2 cell viability recovered to above 100% of control level. In contrast with boiling water, where NP release was low, the toxic impact of released NPs on intestinal cell redox was minimal. Thus, EGCG increased the MTT response under the tested conditions; this preliminary effect may be associated with the known antioxidant activity of EGCG and/or with EGCG–nanoplastic interactions that alter particle surface behavior, such as binding and aggregation, thereby potentially reducing biological interactions.[47,48] However, these mechanisms require direct verification in future work. Additional endpoints, including ROS, TEER, and LDH, will be important in future studies to provide mechanistic insight. These observations underscore the importance of accounting for both the source of plastic exposure and the presence of polyphenolic compounds, such as EGCG, when assessing the effect of using microwave heating on tea beverages.

Dietary intake pathways and food–plastic interactions: implications for nanoplastic exposure, food safety, and environmental health

MNPs can enter the human diet from various sources, such as contaminated food products, food processing, and packaging materials. For example, seafood accumulates MNPs from contaminated marine environments, serving as a key food source. Drinking water and beverages contained in plastic bottles also contributes to exposure due to the release of MNPs. Similarly, heating food in plastic containers, particularly in microwaves, can accelerate the release of microplastics into foods, such as ready-to-eat meals. Fig. 5 (top panel) illustrates the estimated daily dietary intake of microplastics across different countries. Regions with higher plastic consumption in food packaging, seafood-heavy diets, and greater environmental plastic pollution tend to show higher microplastic ingestion rates.[43] For instance, countries in Southeast Asia, such as Indonesia, Malaysia, and the Philippines, report the highest microplastic ingestion rates. In fact, Indonesians eat about 15 grams of microplastics every month, more than any other country, and by comparison, dietary intake in North America was roughly 2.2 grams per month. Given the growing health and environmental concerns surrounding MNPs, understanding the foods consumed that are also contained in plastic packaging and the factors that may influence this process is critical for risk mitigation and developing effective strategies.

We provide new evidence that the major tea polyphenol, EGCG, significantly influences nanoplastic release under thermal exposure. Our study highlights significant implications for food safety and public health by demonstrating that polyphenol-rich beverages, such as tea containing EGCG, can enhance nanoplastic release from plastic cups, particularly under microwave heating. This finding could challenge existing food packaging safety assessments, which primarily focus on chemical additives or nanomaterial migration limits without accounting for real-world interactions between food components and plastic materials. From a practical perspective, our findings contribute to ongoing discussions about food packaging safety and consumer practices. While plastics labeled as "microwave-safe" are widely used, our study suggests that other factors, such as heating conditions, food composition, and repeated use could also influence the extent of MNP release.

Interestingly, while EGCG enhanced NP release, we also demonstrated protective antioxidant effects against NP-induced cellular stress in our *in vitro* intestinal cell-based model. This raises important questions about how food matrix components interact with nanoplastics in the digestive system and whether the interaction could affect NP intestinal health. It is also important to explore whether other dietary antioxidants have similar protective effects and how different types of plastics behave under various food preparation conditions. Our research findings emphasize the importance of a broader understanding of real-world food–plastic interactions in assessing MNP dietary intake and highlight the need for further research on dietary strategies or common practices to mitigate NP potential toxicity. One example is the common practice in parts of Asia of consuming hot tea from reusable plastic cups on a regular basis. Here, the daily intake of EGCG from tea and exposure to ingested NPs are cumulative and interconnected.

The lower panel of Fig. 5 presents a flowchart detailing the factors that impact MNP release from plastic packaging, the potential health and environmental consequences, and pathways to developing safer packaging solutions. Several key factors contribute to MNP migration into food, including the composition of the food/beverage, the type and condition of plastic packaging, and environmental conditions such as heat, acidity, and UV exposure. Once ingested, these particles may cause negative environmental impacts and pose health risks, such as oxidative stress and inflammation, which are linked to broader concerns regarding chronic, long-term human exposure. To support risk assessment, further research innovation is necessary for studying the interactions between food/beverage components and packaging materials under real-world conditions. A better understanding of these factors could better support the development of safer and more sustainable packaging materials while ensuring that food/bever-

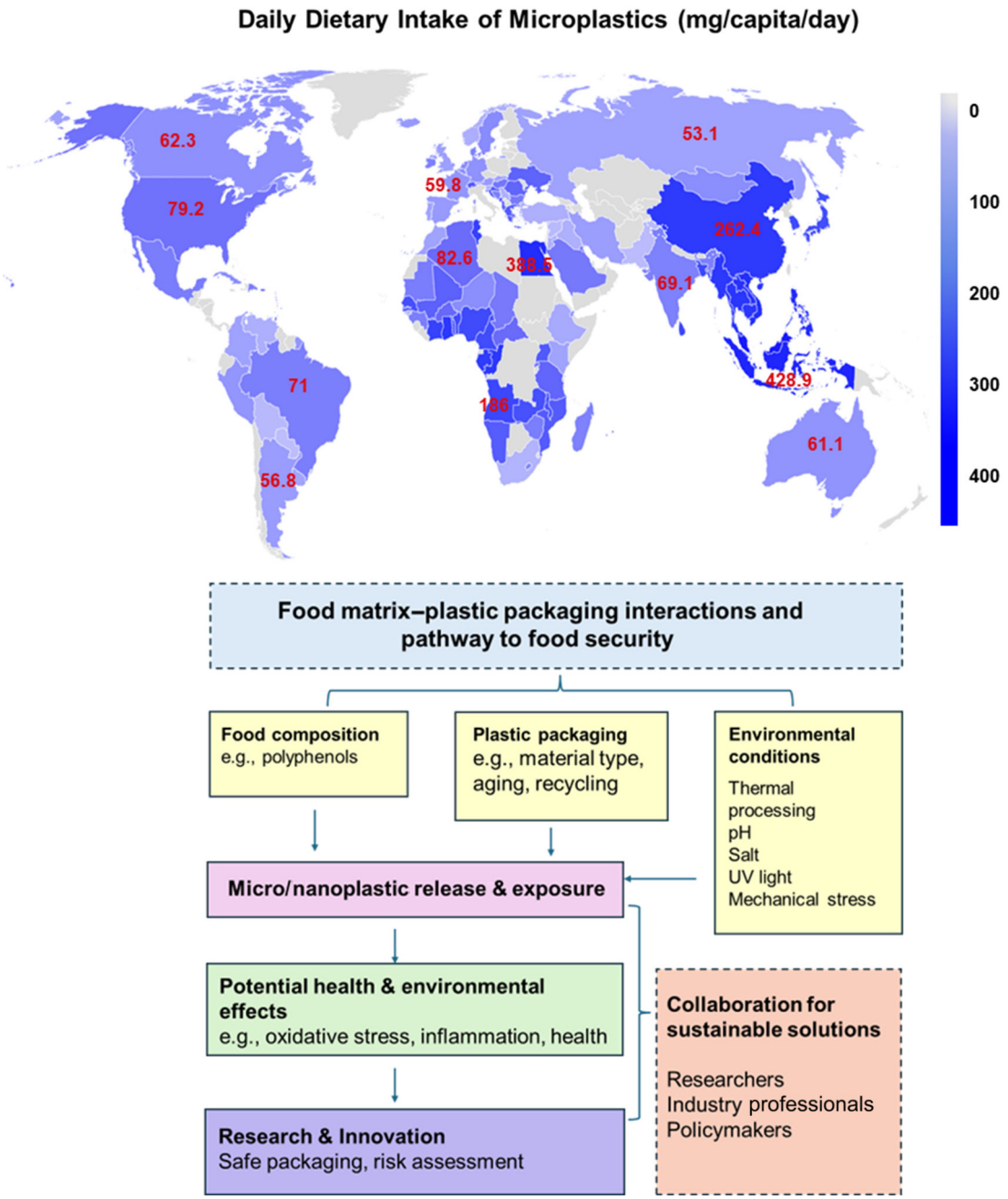

Fig. 5 Global dietary intake of microplastics (mg per capita per day) and conceptual framework illustrating the interactions between food matrices and plastic packaging and their implications for food safety and security. The map shows estimated daily microplastic intake across different regions, emphasizing the worldwide prevalence of plastic particle exposure. The schematic below highlights key contributing factors, including food composition (*e.g.*, polyphenols), packaging characteristics (*e.g.*, material type, aging, and recycling), and environmental conditions (*e.g.*, thermal processing, pH, UV light, and mechanical stress), that influence micro/nanoplastic release and human exposure. The resulting health and environmental effects, such as oxidative stress and inflammation, highlight the need for continued research and innovation in safe packaging design, risk assessment, and cross-sector collaboration among researchers, industry professionals, and policymakers to develop sustainable solutions.

age preparation methods minimize unintended exposure to MNPs. Collaborative efforts between researchers, industry professionals, and regulatory bodies may help guide future innovations in food packaging and food safety assessments, ultimately benefiting both consumer health and environmental sustainability.

Conclusions

This study establishes a robust analytical framework for quantifying nanoplastics released from plastic cups containing polyphenols during heating treatments. We provide new evidence that the major tea polyphenol, EGCG, significantly influ-

ences nanoplastic release under thermal exposure. EGCG greatly increased nanoparticle release, particularly during microwave heating, while simultaneously mitigating nanoplastic-induced cytotoxicity in differentiated Caco-2 cells. Repeated use of PS cups in boiling water led to cumulative nanoparticle release, emphasizing long-term exposure concerns associated with plastic reuse. These findings reveal complex chemical and physical interactions among beverage composition, packaging materials, and environmental factors that shape nanoplastic release and exposure pathways. By integrating advanced SERS detection with toxicological assessment, this work advances the current understanding of MNP exposure mechanisms at the food–environment interface. The study provides novel insights into contaminant release dynamics, exposure risk assessment, and the need for safer, more sustainable materials in food contact applications. Future research should focus on the interplay between diverse food components and packaging materials, which will be critical to mitigating unintended nanoplastic exposure and promoting public and environmental health.

Author contributions

The manuscript was written through contributions from all authors. All authors have given approval to the final version of the manuscript.

Conflicts of interest

There are no conflicts to declare.

Data availability

The data supporting this article have been included as part of the supplementary information (SI). Supplementary information: SERS detection of nanoplastics, effect of heating on SERS detection, and raw SERS spectra of NP release across different conditions (PDF). See DOI: https://doi.org/10.1039/d6nr00796a.

Acknowledgements

This work was supported by the UBC Faculty of Land and Food Systems/Start-Up Funds (AWD-020249 UBCLANDF 2022), the Natural Sciences and Engineering Research Council of Canada (NSERC) Discovery Grants Program (RGPIN-2023-04100) and the NSERC Discovery Grants Program–Discovery Launch Supplement (DGECR-2023-00386). We acknowledge the Canada Foundation for Innovation and John R. Evans Leaders Fund (CFI-JELF #44768) and the British Columbia Knowledge Development Fund (BCKDF). We also thank V. Pringle from the UBC Bioimaging Facility (RRID: SCR_021304) for completing TEM.

References

1 W. Li, C. Wu, Z. Xiong, C. Liang, Z. Li, B. Liu, Q. Cao, J. Wang, J. Tang and D. Li, Self-Driven Magnetorobots for Recyclable and Scalable Micro/Nanoplastic Removal from Nonmarine Waters, *Sci. Adv.*, 2022, **8**(45), eade1731, DOI: 10.1126/sciadv.ade1731.

2 H. Ye, X. Zheng, H. Yang, M. Kowal, T. Seifried, G. P. Singh, K. Aayush, G. Gao, E. Grant, D. Kitts, R. Yada and T. Yang, Rapid Detection of Micro/Nanoplastics Via Integration of Luminescent Metal Phenolic Networks Labeling and Quantitative Fluorescence Imaging in A Portable Device, *ChemRxiv*, 2023, preprint. DOI: 10.26434/chemrxiv-2023-jnbm1.

3 A. Stubbins, K. L. Law, S. E. Muñoz, T. S. Bianchi and L. Zhu, Plastics in the Earth System, *Science*, 2021, **373**(6550), 51–55, DOI: 10.1126/science.abb0354.

4 K. Yin, Y. Wang, H. Zhao, D. Wang, M. Guo, M. Mu, Y. Liu, X. Nie, B. Li, J. Li and M. Xing, A Comparative Review of Microplastics and Nanoplastics: Toxicity Hazards on Digestive, Reproductive and Nervous System, *Sci. Total Environ.*, 2021, **774**, 145758, DOI: 10.1016/j.scitotenv.2021.145758.

5 M. Hu and D. Palić, Micro- and Nano-Plastics Activation of Oxidative and Inflammatory Adverse Outcome Pathways, *Redox Biol.*, 2020, **37**, 101620, DOI: 10.1016/j.redox.2020.101620.

6 C. Fang, Y. Luo and R. Naidu, Microplastics and Nanoplastics Analysis: Options, Imaging, Advancements and Challenges, *TrAC, Trends Anal. Chem.*, 2023, **166**, 117158, DOI: 10.1016/j.trac.2023.117158.

7 K. Shi, H. Zhang, Y. Yang, Y. Huang, J. Gao, J. Zhang, G. Kan, Y. Jiang and J. Jiang, Efficient Extraction and Analysis of Nanoplastics by Ionic Liquid-Assisted Cloud-Point Extraction Coupled with Electromagnetic Heating Pyrolysis Mass Spectrometry, *Anal. Chem.*, 2024, **96**(11), 4514–4520, DOI: 10.1021/acs.analchem.3c05208.

8 H. Cai, E. G. Xu, F. Du, R. Li, J. Liu and H. Shi, Analysis of Environmental Nanoplastics: Progress and Challenges, *Chem. Eng. J.*, 2021, **410**, 128208, DOI: 10.1016/j.cej.2020.128208.

9 X. Zhang, K. Shi, Y. Liu, Y. Chen, K. Yu, Y. Wang, H. Zhang and J. Jiang, Rapid and Efficient Method for Assessing Nanoplastics by an Electromagnetic Heating Pyrolysis Mass Spectrometry, *J. Hazard. Mater.*, 2021, **419**, 126506, DOI: 10.1016/j.jhazmat.2021.126506.

10 C. Xiang, J. Gao, H. Ye, G. Ren, X. Ma, H. Xie, S. Fang, Q. Lei and W. Fang, Development of Ovalbumin-Pectin Nanocomplexes for Vitamin D3 Encapsulation: Enhanced Storage Stability and Sustained Release in Simulated Gastrointestinal Digestion, *Food Hydrocoll.*, 2020, **106**, 105926, DOI: 10.1016/j.foodhyd.2020.105926.

11 H. Ye, T. Chen, M. Huang, G. Ren, Q. Lei, W. Fang and H. Xie, Exploration of the Microstructure and Rheological Properties of Sodium Alginate-Pectin-Whey Protein Isolate Stabilized B-Carotene Emulsions: To Improve Stability and Achieve Gastrointestinal Sustained Release, *Foods*, 2021, **10**(9), 1991, DOI: 10.3390/foods10091991.

12 Z. Li, K. Han, A. Zhang, T. Wang, Z. Yan, Z. Ding, Y. Shen, M. Zhang and W. Zhang, Honeycomb-like AgNPs@TiO2 Array SERS Sensor for the Quantification of Micro/Nanoplastics in the Environmental Water Samples, *Talanta*, 2024, **266**, 125070, DOI: 10.1016/j.talanta.2023.125070.

13 J. Leonard, H. C. Koydemir, V. S. Koutnik, D. Tseng, A. Ozcan and S. K. Mohanty, Smartphone-Enabled Rapid Quantification of Microplastics, *J. Hazard. Mater. Lett.*, 2022, **3**, 100052, DOI: 10.1016/j.hazl.2022.100052.

14 H. Ye, G. Gao and T. Yang, *Quantitative and Rapid Detection of Nanoplastics Labeled by Luminescent Metal Phenolic Networks Using Surface Enhanced Raman Scattering*, Rochester, NY, 2024. DOI: 10.2139/ssrn.4696808.

15 Z. Lin, J. Zhou, Y. Qu, S. Pan, Y. Han, R. P. M. Lafleur, J. Chen, C. Cortez-Jugo, J. J. Richardson and F. Caruso, Luminescent Metal-Phenolic Networks for Multicolor Particle Labeling, *Angew. Chem., Int. Ed.*, 2021, **60**(47), 24968–24975, DOI: 10.1002/anie.202108671.

16 L. M. Hernandez, E. G. Xu, H. C. E. Larsson, R. Tahara, V. B. Maisuria and N. Tufenkji, Plastic Teabags Release Billions of Microparticles and Nanoparticles into Tea, *Environ. Sci. Technol.*, 2019, **53**(21), 12300–12310, DOI: 10.1021/acs.est.9b02540.

17 L. M. Hernandez, E. G. Xu, H. C. E. Larsson, R. Tahara, V. B. Maisuria and N. Tufenkji, Plastic Teabags Release Billions of Microparticles and Nanoparticles into Tea, *Environ. Sci. Technol.*, 2019, **53**(21), 12300–12310, DOI: 10.1021/acs.est.9b02540.

18 D.-H. Lee, W.-H. Kim, K. Lee, I. Na, X. Fu, H. W. Jeong, J.-O. Chung, J. Roh, W. Kim and S.-M. Shim, Green Tea Extracts Rich in Epicatechins Inducing Aggregation and Inhibiting Absorption of Amine Surface Functionalized Polystyrene Microplastics *in Vitro* Mimick System, *J. Hazard. Mater. Adv.*, 2024, **15**, 100437, DOI: 10.1016/j.hazadv.2024.100437.

19 H. Xie, X. Luo, Y. Gao, M. Huang, G. Ren, R. Zhou, Y. Sun, H. Ye, Q. Lei, W. Fang and Y.-Q. Xu, Co-Encapsulation of *Lactobacillus Plantarum* and EGCG: A Promising Strategy to Increase the Stability and Lipid-Lowering Activity, *Food Hydrocoll.*, 2024, **151**, 109768, DOI: 10.1016/j.foodhyd.2024.109768.

20 C. Hu and D. D. Kitts, Evaluation of Antioxidant Activity of Epigallocatechin Gallate in Biphasic Model Systems in Vitro, *Mol. Cell. Biochem.*, 2001, **218**(1), 147–155, DOI: 10.1023/A:1007220928446.

21 I. C. W. Arts, B. van de Putte and P. C. H. Hollman, Catechin Contents of Foods Commonly Consumed in The Netherlands. 2. Tea, Wine, Fruit Juices, and Chocolate Milk, *J. Agric. Food Chem.*, 2000, **48**(5), 1752–1757, DOI: 10.1021/jf000026+.

22 A. G. Atanasov, S. M. Sabharanjak, G. Zengin, A. Mollica, A. Szostak, M. Simirgiotis, Ł. Huminiecki, O. K. Horbanczuk, S. M. Nabavi and A. Mocan, Pecan Nuts: A Review of Reported Bioactivities and Health Effects, *Trends Food Sci. Technol.*, 2018, **71**, 246–257, DOI: 10.1016/j.tifs.2017.10.019.

23 H. Ye, E. B. Esfahani, I. Chiu, M. Mohseni, G. Gao and T. Yang, Quantitative and Rapid Detection of Nanoplastics Labeled by Luminescent Metal Phenolic Networks Using Surface-Enhanced Raman Scattering, *J. Hazard. Mater.*, 2024, **470**, 134194, DOI: 10.1016/j.jhazmat.2024.134194.

24 H. Ye, X. Zheng, H. Yang, M. D. Kowal, T. M. Seifried, G. P. Singh, K. Aayush, G. Gao, E. Grant, D. Kitts, R. Y. Yada and T. Yang, Cost-Effective and Wireless Portable Device for Rapid and Sensitive Quantification of Micro/Nanoplastics, *ACS Sens.*, 2024, **9**(9), 4662–4670, DOI: 10.1021/acssensors.4c00957.

25 M. D. Kowal, T. M. Seifried, C. C. Brouwer, H. Tavakolizadeh, E. Olsén and E. Grant, Electrophoretic Deposition Interferometric Scattering Mass Photometry, *ACS Nano*, 2024, **18**(15), 10388–10396, DOI: 10.1021/acsnano.3c09221.

26 P. Kumar, A. Nagarajan and P. D. Uchil, Analysis of Cell Viability by the MTT Assay, *Cold Spring Harb. Protoc.*, 2018, **6**, 469–471, DOI: 10.1101/pdb.prot095505.

27 L.-A. Wu, W.-E. Li, D.-Z. Lin and Y.-F. Chen, Three-Dimensional SERS Substrates Formed with Plasmonic Core-Satellite Nanostructures, *Sci. Rep.*, 2017, **7**(1), 13066, DOI: 10.1038/s41598-017-13577-9.

28 S. Huh, J. Park, Y. S. Kim, K. S. Kim, B. H. Hong and J.-M. Nam, UV/Ozone-Oxidized Large-Scale Graphene Platform with Large Chemical Enhancement in Surface-Enhanced Raman Scattering, *ACS Nano*, 2011, **5**(12), 9799–9806, DOI: 10.1021/nn204156n.

29 Y. Zhao, L. Xu, F. Kong and L. Yu, Design and Preparation of Poly(Tannic Acid) Nanoparticles with Intrinsic Fluorescence: A Sensitive Detector of Picric Acid, *Chem. Eng. J.*, 2021, **416**, 129090, DOI: 10.1016/j.cej.2021.129090.

30 Z. Lin, J. Zhou, Y. Qu, S. Pan, Y. Han, R. P. M. Lafleur, J. Chen, C. Cortez-Jugo, J. J. Richardson and F. Caruso, Luminescent Metal-Phenolic Networks for Multicolor Particle Labeling, *Angew. Chem., Int. Ed.*, 2021, **60**(47), 24968–24975, DOI: 10.1002/anie.202108671.

31 O. Mazaheri, M. S. Alivand, A. Zavabeti, S. Spoljaric, S. Pan, D. Chen, F. Caruso, H. C. Suter and K. A. Mumford, Assembly of Metal–Phenolic Networks on Water-Soluble Substrates in Nonaqueous Media, *Adv. Funct. Mater.*, 2022, **32**(24), 2111942, DOI: 10.1002/adfm.202111942.

32 S. E. J. Bell and N. M. S. Sirimuthu, Quantitative Surface-Enhanced Raman Spectroscopy, *Chem. Soc. Rev.*, 2008, **37**(5), 1012, DOI: 10.1039/b705965p.

33 H. Ye, S. Jiang, Y. Yan, B. Zhao, E. Grant, D. Kitts, R. Yada, A. Pratap-Singh, A. Baldelli and T. Yang, Integrating Metal Phenolic Networks-Mediated Separation and Machine Learning-Aided SERS for High-Precision Quantification and Classification of Nanoplastics, *ChemRxiv*, 2024, preprint. DOI: 10.26434/chemrxiv-2024-kn4zj.

34 G. Liu, J. Wang, M. Wang, R. Ying, X. Li, Z. Hu and Y. Zhang, Disposable Plastic Materials Release Microplastics and Harmful Substances in Hot Water, *Sci. Total Environ.*, 2022, **818**, 151685, DOI: 10.1016/j.scitotenv.2021.151685.

35 L. M. Hernandez, E. G. Xu, H. C. E. Larsson, R. Tahara, V. B. Maisuria and N. Tufenkji, Plastic Teabags Release Billions of Microparticles and Nanoparticles into Tea, *Environ. Sci. Technol.*, 2019, **53**(21), 12300–12310, DOI: 10.1021/acs.est.9b02540.

36 Y. Y. Hee, K. Weston and S. Suratman, The Effect of Storage Conditions and Washing on Microplastic Release from Food and Drink Containers, *Food Packag. Shelf Life*, 2022, **32**, 100826, DOI: 10.1016/j.fpsl.2022.100826.

37 Z.-Y. Chen, Q. Y. Zhu, D. Tsang and Y. Huang, Degradation of Green Tea Catechins in Tea Drinks, *J. Agric. Food Chem.*, 2001, **49**(1), 477–482, DOI: 10.1021/jf000877h.

38 H. Xie, X. Luo, Y. Gao, M. Huang, G. Ren, R. Zhou, Y. Sun, H. Ye, Q. Lei, W. Fang and Y.-Q. Xu, Co-Encapsulation of *Lactobacillus Plantarum* and EGCG: A Promising Strategy to Increase the Stability and Lipid-Lowering Activity, *Food Hydrocoll.*, 2024, **151**, 109768, DOI: 10.1016/j.foodhyd.2024.109768.

39 W. Zhao, X. Liang, X. Wang, S. Wang, L. Wang and Y. Jiang, Chitosan Based Film Reinforced with EGCG Loaded Melanin-like Nanocomposite (EGCG@MNPs) for Active Food Packaging, *Carbohydr. Polym.*, 2022, **290**, 119471, DOI: 10.1016/j.carbpol.2022.119471.

40 Y. Wang, M. Wang, Q. Wang, T. Wang, Z. Zhou, M. Mehling, T. Guo, H. Zou, X. Xiao, Y. He, X. Wang, O. J. Rojas and J. Guo, Flowthrough Capture of Microplastics through Polyphenol-Mediated Interfacial Interactions on Wood Sawdust, *Adv. Mater.*, 2023, **35**(36), 2301531, DOI: 10.1002/adma.202301531.

41 H. Zhu, X. Ma, J. Y. Kong, M. Zhang and H. I. Kenttämaa, Identification of Carboxylate, Phosphate, and Phenoxide Functionalities in Deprotonated Molecules Related to Drug Metabolites via Ion–Molecule Reactions with Water and Diethylhydroxyborane, *J. Am. Soc. Mass Spectrom.*, 2017, **28**(10), 2189–2200, DOI: 10.1007/s13361-017-1713-0.

42 L. Zhang, Y. Liu and Y. Wang, Deprotonation Mechanism of Methyl Gallate: UV Spectroscopic and Computational Studies, *Int. J. Mol. Sci.*, 2018, **19**(10), 3111, DOI: 10.3390/ijms19103111.

43 F. Awaja, S. Zhang, M. Tripathi, A. Nikiforov and N. Pugno, Cracks, Microcracks and Fracture in Polymer Structures: Formation, Detection, Autonomic Repair, *Prog. Mater. Sci.*, 2016, **83**, 536–573, DOI: 10.1016/j.pmatsci.2016.07.007.

44 D. Xu, Y. Ma, X. Han and Y. Chen, Systematic Toxicity Evaluation of Polystyrene Nanoplastics on Mice and Molecular Mechanism Investigation about Their Internalization into Caco-2 Cells, *J. Hazard. Mater.*, 2021, **417**, 126092, DOI: 10.1016/j.jhazmat.2021.126092.

45 M. Llorca and M. Farré, Current Insights into Potential Effects of Micro-Nanoplastics on Human Health by in-Vitro Tests, *Front. Toxicol.*, 2021, **3**, 752140, DOI: 10.3389/ftox.2021.752140.

46 V. Mattioda, V. Benedetti, C. Tessarolo, F. Oberto, A. Favole, M. Gallo, W. Martelli, M. I. Crescio, E. Berio, L. Masoero, A. Benedetto, M. Pezzolato, E. Bozzetta, C. Grattarola, C. Casalone, C. Corona and F. Giorda, Pro-Inflammatory and Cytotoxic Effects of Polystyrene Microplastics on Human and Murine Intestinal Cell Lines, *Biomolecules*, 2023, **13**(1), 140, DOI: 10.3390/biom13010140.

47 D.-H. Lee, W.-H. Kim, K. Lee, I. Na, X. Fu, H. W. Jeong, J.-O. Chung, J. Roh, W. Kim and S.-M. Shim, Green Tea Extracts Rich in Epicatechins Inducing Aggregation and Inhibiting Absorption of Amine Surface Functionalized Polystyrene Microplastics *in Vitro* Mimick System, *J. Hazard. Mater. Adv.*, 2024, **15**, 100437, DOI: 10.1016/j.hazadv.2024.100437.

48 B. N. Singh, S. Shankar and R. K. Srivastava, Green Tea Catechin, Epigallocatechin-3-Gallate (EGCG): Mechanisms, Perspectives and Clinical Applications, *Biochem. Pharmacol.*, 2011, **82**(12), 1807–1821, DOI: 10.1016/j.bcp.2011.07.093.